Comparison of methods for calculating the properties of intramolecular hydrogen bonds. Excited state proton transfer

Tapas Kar, Steve Scheiner,[a] and Martin Čuma[b]
Department of Chemistry, Southern Illinois University, Carbondale, Illinois 62901-4409

(Received 1 February 1999; accepted 13 April 1999)

A series of molecules related to malonaldehyde, containing an intramolecular H-bond, are used as the testbed for a variety of levels of *ab initio* calculation. Of particular interest are the excitation energies of the first set of valence excited states, $n\pi^*$ and $\pi\pi^*$, both singlet and triplet, as well as the energetics of proton transfer in each state. Taking coupled cluster results as a point of reference, configuration interaction-singles–second-order Møller–Plesset (CIS–MP2) excitation energies are too large, as are CIS to a lesser extent, although these approaches successfully reproduce the order of the various states. The same may be said of complete active space self-consistent-field (CASSCF), which is surprisingly sensitive to the particular choice of orbitals included in the active space. Complete active space–second-order perturbation theory (CASPT2) excitation energies are rather close to coupled cluster singles and doubles (CCSD), as are density functional theory (DFT) values. CASSCF proton transfer barriers are large overestimates; the same is true of CIS to a lesser extent. MP2, CASPT2, and DFT barriers are closer to coupled cluster results, although yielding slight underestimates. © *1999 American Institute of Physics.* [S0021-9606(99)30226-9]

INTRODUCTION

Recent years have witnessed an accelerating interest in the problem of excited state proton transfer (ESPT). This growth has been fueled by a wide range of potential applications, including lasers,[1,2] energy/data storage devices and optical switching,[3,4] Raman filters and hard-scintillation counters,[5] polymer photostabilizers,[6] and triplet quenchers.[7] Other uses center about electroluminescent materials with photochemical stability, resistance to thermal degradation, and low self-absorption and LED materials.[8]

Our current understanding of the proton transfer process in the ground electronic state was achieved largely through a cooperative effort, wherein experimental information was complemented by data and concepts derived from quantum chemical calculations of model systems.[9–13] Advances in experimental techniques have made the excited state process more amenable to detailed study in recent years, and a wealth of data now exists.[14–21] Unfortunately, the development of *ab initio* methods that can reliably treat excited states has lagged behind the capability to study the ground electronic state. Nonetheless, genuine advances have been made, and such theoretical studies are beginning to proliferate.[22–32]

There exist a number of different theoretical methods that are capable in principle of treating a proton transfer in a given excited state. In general, each previous calculation has applied one of these particular theoretical approaches, within the context of a different basis set, to a different chemical system. As a result, it is difficult to gauge the reliability and accuracy of any one given set of calculations; when different methods are used on similar systems one is confronted with the potentially bewildering problem of determining which set of data is most credible.

As an example, a multiconfiguration self-consistent-field (MCSCF) study of o-hydroxybenzaldehyde[33] had difficulty predicting whether a proton would transfer between the two oxygen atoms in the first $^1\pi\pi^*$ state; the H-bond geometry of this state was rather similar to S_o. In contrast, complete active space SCF (CASSCF) computations of this same state[34] suggested the enol and keto tautomers are nearly equally stable with an energy barrier of some 15 kcal/mol separating them. Still different conclusions were derived from a complete active space–second-order perturbation theory (CASPT2) calculation by the same authors, which indicated that neither the keto nor enol represents a minimum, but rather that the proton sits somewhere between the two oxygen atoms in the optimum geometry. Another theoretical approach predicted the keto as the more stable tautomer of the two, but with a low to nonexistent barrier separating them.[31]

The problem is exacerbated by the paucity of experimental information that is accurate and quantitative enough to act as a reliable yardstick by which to measure the performance of the calculations on the excited-state properties of the molecules under study. In the absence of such an experimental gauge, probably the next best test is that of internal consistency: are the theoretical calculations consistent amongst themselves? What is missing at this point, then, is a comprehensive and systematic comparison of several different theoretical methods on the same system or set of systems. Such a comparison would provide information about the level of reliability of each method. Certain methods might, for example, consistently underestimate the energy barrier to proton transfer, others might have a propensity to favor one

[a]Electronic mail: scheiner@chem.siu.edu
[b]Present address: Dept. of Chemistry, University of Utah, Salt Lake City, Utah 84112.

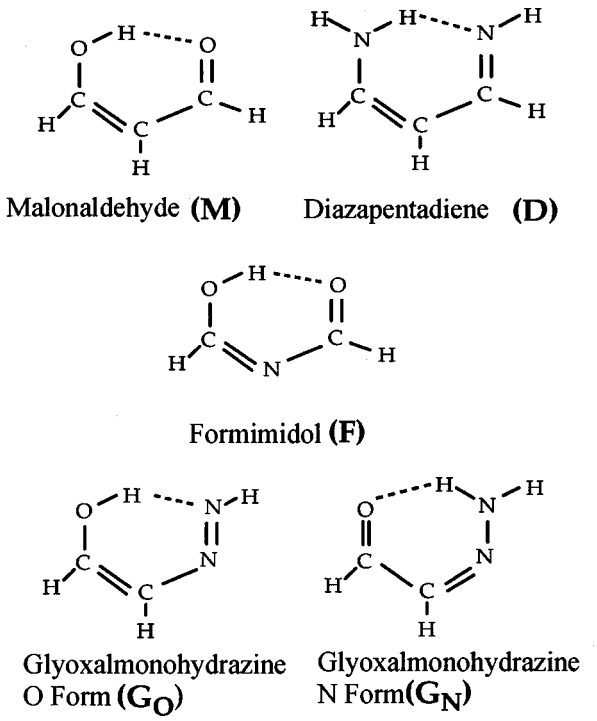

FIG. 1. Molecules investigated, including their abberviations.

tautomer over the other on a consistent basis. Indeed, there may be some methods that are virtually worthless as the data they provide are not consistent enough to be of use. It is the central goal of the present communication to perform such a comparison. The successful identification of theoretical methods that can reliably treat the excited state proton transfer process would enable calculations to serve a genuine predictive function, and to help guide workers toward key experiments.

METHODS

The molecules considered in this work are illustrated in Fig. 1. Malonaldehyde (**M**) contains an intramolecular H-bond connecting two O atoms, which are in turn part of a five-atom conjugated ring.[35] The variants of M pictured in Fig. 1 are all isoelectronic with malonaldehyde. Replacement of the two O atoms by NH leads to the diazapentadiene molecule (**D**).[36] A more minor variant on the M theme is formimidol (**F**) which is identical to malonaldehyde, with the exception of the replacement of the central CH group by a nitrogen atom.[37] In each of the aforementioned systems, the proton transfer is symmetric in the sense that the product of the transfer is equivalent to the reactant pictured in Fig. 1. Such is not the case if only one oxygen atom of malonaldehyde is replaced by nitrogen. The tautomer of glyoxalmonohydrazine (**G**), wherein the bridging hydrogen is covalently bound to the oxygen, $\mathbf{G_O}$, is quite different from the $\mathbf{G_N}$ tautomer resulting from transfer of the hydrogen across to the nitrogen atom.[38] For each system, two configurations were considered, both of which are planar. The equilibrium geometries depicted in Fig. 1 belong to the C_s point group. In order to assess the barrier to proton transfer, the transition state to this process was identified; these more highly symmetric transition states belong to the C_{2v} point group, with the exception of the less symmetric glyoxalmonohydrazine, where the transition state belongs to the C_s point group.

Results reported were obtained with the 4-31G basis set[39] and with 6-31+G**;[40,41] the latter contains polarization functions on all atoms, and diffuse functions on nonhydrogen atoms. While 6-31+G** is of course preferable to the smaller 4-31G, it might not always be possible to apply an extended basis, particularly when the molecule under scrutiny is much larger than those considered here. For that reason, we compare 4-31G results with 6-31+G**, to act as a guide to errors that might be incurred by workers forced to restrict their calculations to the smaller set. The comparison also acts as a means of elucidating the effects of polarization functions to the excited state properties of the pertinent molecules.

Electronic states considered in addition to the ground state were the first few excited valence singlets and triplets, namely $\pi\pi^*$ and $n\pi^*$. Geometries were obtained by a full optimization at the configuration interaction-singles (CIS) level[42] of each molecule in each given electronic state. In addition to CIS, energies were computed at various other levels of theory. Complete active space self-consistent-field (CASSCF) calculations[43,44] were performed using two different active spaces: Correlation of six electrons within seven orbitals is denoted CASSCF(6/7), while CASSCF(8/8) correlates eight electrons within eight orbitals. (The details of the specific orbitals are discussed below.) Second-order perturbation theory was used to add correlation effects to the aforementioned CASSCF wave functions. The complete active space–second-order perturbation theory (CASPT2) (m/n) nomenclature[45,46] refers to the same values of m electrons in n orbitals as in CAS(m/n). The complete active space calculations were carried out using the MOLCAS-3 *ab initio* package.[47] For purposes of comparison, the same geometries were subjected to coupled-cluster calculations both at the singles/doubles level (CCSD),[48–50] and with added extrapolation to triples, CCSD(T).[51] Also considered is the density functional theory, DFT, approach,[52,53] the reliability of which remains largely untested for excited states. Becke's three parameter functional was used to model the exchange[54] and correlation was included via the functionals of Lee, Yang, and Parr[55] (B3LYP). CIS, coupled-cluster, and DFT computations were performed using GAUSSIAN-94[56] and 98.[57]

RESULTS

The complete active space formalism contains a certain amount of ambiguity in terms of which particular electrons and orbitals are chosen for inclusion. For this reason, some preliminary exploration of this question was conducted here. For example, within the context of the CASSCF(6/7) study of malonaldehyde, three different schemes were considered. As indicated by the first two columns of Table I, the six electrons are contained in one occupied σ orbital (a' in this planar molecule) and two π orbitals (a''). With regard to which four virtual orbitals are added to these three originally doubly occupied orbitals for purposes of correlation, the three choices included zero, one, or two σ^* orbitals, respectively; the remainder of the four orbitals are of π^* type (4, 3,

TABLE I. Comparison of CASSCF energies, equilibrium geometry.

	Active occupied orbitals		Active unoccupied orbitals		E (CASSCF), au	
	$a'(\sigma)$	$a''(\pi)$	$a'(\sigma^*)$	$a''(\pi^*)$	4-31G	6-31+G**
Malonaldehyde (6/7)						
	1	2	0	4	−265.304 93	−265.710 76
	1	2	1	3	−265.342 66	−265.735 54
	1	2	2	2	−265.340 99	−265.721 83
Malonaldehyde (8/8)						
	1	3	0	4	−265.316 36	−265.721 40
	1	3	1	3	−265.352 13	−265.753 44
	1	3	2	2	−265.342 26	−265.744 38
Diazapentadiene (6/7)						
	1	2	0	4	−225.689 64	−226.042 69
	1	2	1	3	−225.719 38	−226.068 85
	1	2	2	2	−225.718 21	−226.067 97
Diazapentadiene (8/8)						
	1	3	0	4	−225.700 60	−226.052 76
	1	3	1	3	−225.728 57	−226.078 26
	1	3	2	2	−225.720 30	−226.064 71
Glyoxalmonohydrazine $\mathbf{G_N}$ (6/7)						
	1	2	0	4	−261.437 78	−261.846 67
	1	2	1	3	−261.475 05	−261.876 83
Glyoxalmonohydrazine $\mathbf{G_N}$ (8/8)						
	1	3	0	4	−261.450 27	−261.858 31
	1	3	1	3	−261.484 28	−261.888 04
Glyoxalmonohydrazine $\mathbf{G_O}$ (6/7)						
	1	2	0	4	−261.413 53	−261.833 13
	1	2	1	3	−261.449 49	−261.863 08
Glyoxalmonohydrazine $\mathbf{G_O}$ (8/8)						
	1	3	0	4	−261.424 79	−261.841 99
	1	3	1	3	−261.458 90	−261.873 02

and 2). The CASSCF energies of malonaldehyde are most negative for the second choice, i.e., one σ^* and three π^* virtual orbitals. This preference is valid for both the 4-31G and larger 6-31+G** basis sets. The next three rows of Table I indicate that the same choice of virtuals provides the lowest energy for the (8/8) set, wherein the eight electrons originate in one σ and three π occupied MOs. Turning now to other molecules, this same pattern is repeated for diazapentadiene, where again the single σ^* orbital, coupled with three π^* orbitals, leads to the lowest energy. This choice of virtual orbitals is optimal for both the 4-31G and 6-31 +G** basis sets, and both (6/7) and (8/8) levels. A scan of the remaining data in Table I illustrates that the optimal choice of virtual orbitals to include in the correlated space of the molecules discussed here is the same set of one σ^* orbital, plus three π^* orbitals.

The transition states to proton transfer, with the proton midway between the two pertinent atoms, has a higher degree of symmetry than the equilibrium structures. In the C_{2v} geometry of the malonaldehyde transition state, for example, the σ orbitals belong to either the a_1 or b_2 representation; likewise the π orbitals fall into either the a_2 or b_1 designation. The highest lying occupied σ orbital is of b_2 symmetry, but various choices were considered for the two or three occupied π orbitals to be included. A greater range of choices is possible in terms of the vacant MOs. Examination of Table II leads to the conclusion that the optimal choice of vacant MOs includes one of a_1 symmetry (σ^*), and three π^* orbitals (one a_2 and two b_1).

In summary, the optimal choice of vacant MOs to be included in the active space for all systems considered, with either basis set, and in either the equilibrium or transition state geometry, consists of one σ^* and three π^* orbitals. This set contains the lone pair MO of the proton-accepting atom, as well as one vacant σ^* counterpart. It is the orbital cluster corresponding to the underlined, i.e., lowest, energies in Tables I and II that have been used in the calculations reported below for each system. The CASPT2 approach of computing dynamic electron correlation takes the CASSCF wave function as its reference. Hence, one can presume that the quality of this perturbational approach is directly related to the value of the reference weight ω. For the active spaces used in the present investigation, ω was found to lie in the range between 0.80 and 0.86.

A modification of the usual CASSCF nomenclature is introduced in this paper. The m and n in CASSCF (m/n) normally refer, respectively, to the number of electrons being correlated and the total number of orbitals (occupied plus vacant) included in their space. So as to provide additional information about which particular orbitals are included, the (ij/kl) notation is introduced wherein i and j denote the number of doubly occupied orbitals of σ and π symmetry, respectively; k and l have a similar meaning for the vacant

TABLE II. Comparison of CASSCF energies of transition state geometries.

Active occupied orbitals				Active unoccupied orbitals				E (CASSCF), au	
a_1 (σ)	b_2 (σ)	a_2 (π)	b_1 (π)	a_1 (σ^*)	b_2 (σ^*)	a_2 (π^*)	b_1 (π^*)	4-31G	6-31+G**
Malonaldehyde (6/7)									
0	1	1	1	0	0	2	2	−265.266 88	−265.680 77
				0	1	1	2	−265.272 38	−265.693 06
				0	1	2	1	−265.271 76	−265.692 50
				1	0	1	2	−265.297 18	−265.707 90
				1	0	2	1	−265.268 30	−265.707 16
Malonaldehyde (8/8)									
0	1	1	2	0	0	2	2	−265.285 09	−265.696 94
				0	0	3	1	−265.267 05	−265.682 26
				0	1	2	1	−265.287 59	−265.698 27
				1	0	1	2	−265.313 24	265.721 22
				1	0	2	1	−265.305 89	−265.715 43
				1	0	3	0	−265.273 58	−265.684 14
Diazapentadiene (6/7)									
0	1	1	1	0	0	2	2	−225.652 63	−226.003 74
				0	1	1	2	−225.663 22	−226.012 64
				0	1	2	1	−225.662 94	−226.007 94
				1	0	1	2	−225.676 90	−226.026 22
				1	0	2	1	−225.676 27	−226.024 87
Diazapentadiene (8/8)									
0	1	1	2	0	0	2	2	−225.670 01	−226.019 22
				0	1	2	1	−225.671 64	−226.021 79
				1	0	1	2	−225.693 03	−226.040 24
				1	0	2	1	−225.685 87	−226.022 41
				1	0	3	0	−225.640 17	−225.995 96

MOs. Hence, $2(i+j)$ is equal to m in the usual notation and the sum of $i+j+k+l$ is equal to n.

Excitation energies

The difference in energy between the ground state of each molecule and the indicated excited state is listed in Table III. The level of theory is listed at the head of each column of data. These values refer to 6-31+G** adiabatic excitation energies in that the geometry of each excited state was optimized. Structures optimized at the CIS level were used for all excited states.

Considering first the malonaldehyde molecule, all levels of theory indicate the same energetic ordering of excited states:

$$^3\pi\pi^* < ^3n\pi^* < ^1n\pi^* < ^1\pi\pi^*,$$

although there are significant quantitative differences in the excitation energies. In comparison with the CCSD results for the two triplets, the CIS–MP2 excitation energies are quite high. The same is true of the CIS value for $^3n\pi^*$, albeit to a lesser extent, whereas the CIS excitation energy for the $^3\pi\pi^*$ state is curiously low. The DFT excitation energies are in surprisingly good agreement with the more reliable CCSD data.

Coupled cluster theory predicts the $^3n\pi^*$ state to be about 2 kcal/mol higher in energy than the corresponding singlet. The other methods indicate a larger energy difference, especially CIS. With respect to the two singlet states, the CASPT2 excitation energies are the smallest of those reported, and most consistent with CCSD and CCSD(T). CIS–MP2 values tend to be the largest, although they are consistent with the CIS and CASSCF data for the $^1\pi\pi^*$ state. With respect to the specifics of the orbitals included in the CASSCF active space, the excitation energies are not terribly sensitive to this parameter. However, there is a curious discrepancy of 15 kcal/mol between the (12/13) and (13/13) excitation energies of the $^3n\pi^*$ state, and another difference of 11 kcal/mol for $^1n\pi^*$. These discrepancies appear to be washed out when correlation is added: the CASPT2 values are less sensitive to the number of orbitals included. It might finally be noted that the coupled-cluster excitation energies of the two triplets reproduce very closely values previously computed at the G2 level.[58]

These patterns are generally repeated for the other molecules in Table III with a number of minor exceptions. There is some question as to which of the two excited singlets of **D** is lower in energy. The CASPT2 calculations indicate that the $^3\pi\pi^*$ state of **F** lies higher in energy than either of the two $n\pi^*$ states, as does the other dynamic correlated method, CIS–MP2. Again, the latter method exaggerates the excitation energies of all four of the states. The same is generally true of the CIS and CASSCF approaches with the exception of the lowest lying $^3\pi\pi^*$ state. The CASPT2 calculations predict a reversal in stability between the two triplets of the $\mathbf{G_O}$ tautomer, a reversal that is not duplicated by the other theoretical methods (with the exception of DFT), nor does it occur in $\mathbf{G_N}$.

Similar computations were carried out with the smaller

TABLE III. Adiabatic excitation energies (kcal/mol) computed for 6-31+G** basis set.

		CASSCF			CASPT2				
State	CIS	(12/13)	(13/13)	CIS–MP2	(12/13)	(13/13)	DFT	CCSD	CCSD(T)
Malonaldehyde (**M**)									
$^3\pi\pi^*$	56.3	69.3	75.5	109.4	71.6	70.9	68.3	71.5	73.7
$^3n\pi^*$	94.5	88.0	103.5	123.0	79.9	76.3	77.8	81.2	83.4
$^1n\pi^*$	110.3	97.5	108.4	126.9	83.6	82.2	79.3	83.3	85.5
$^1\pi\pi^*$	126.1	133.5	134.5	130.6	100.2	94.5			
Diazapentadiene (**D**)									
$^3\pi\pi^*$	60.5	72.3	69.6	109.9	57.6	60.3	60.3	63.7	65.3
$^3n\pi^*$	105.9	101.3	108.0	142.4	86.6	88.3	87.7	91.9	94.5
$^1n\pi^*$	123.5	108.9	115.8	147.8	93.8	97.0	90.2	95.7	98.1
$^1\pi\pi^*$	123.0	130.4	123.4	130.0	93.8	91.9			
Formimidol (**F**)									
$^3\pi\pi^*$	96.5	92.0	92.8	142.6	91.1	92.4	87.9		
$^3n\pi^*$	107.2	115.8	126.4	125.7	87.8	83.4	75.0		
$^1n\pi^*$	118.5	113.9	122.2	124.1	83.6	83.0			
$^1\pi\pi^*$	157.4	147.2	151.9	151.0	117.6	110.6			
Glyoxalmonohydrazine ($\mathbf{G_N}$)									
$^3\pi\pi^*$	52.9	64.8	65.3	105.1	54.6	55.5	54.8		
$^3n\pi^*$	80.3	98.5	104.5	125.9	77.3	76.8	63.4		
$^1n\pi^*$	101.2	98.9	104.9	123.7	81.5	80.8			
$^1\pi\pi^*$	124.3	127.1	122.0	123.6	87.2	81.6			
Glyoxalmonohydrazine ($\mathbf{G_O}$)									
$^3\pi\pi^*$	45.3	56.2	62.4	100.3	46.4	46.9	48.9		
$^3n\pi^*$	46.4	78.1	84.3	100.7	32.0	32.5	42.7		
$^1n\pi^*$	73.6	100.7	106.9	112.6	50.2	50.7			
$^1\pi\pi^*$	119.8	119.7	125.9	124.2	82.0	82.5			

4-31G basis set. The results were much the same as the 6-31+G** data reported in Table III, particularly on a qualitative level. In general, the excitation energies computed with the smaller basis are somewhat lower than the 6-31+G** values. One notable exception to this trend lies in the $^1\pi\pi^*$ state where the pattern reverses and the smaller basis tends toward higher excitation energies. But it should be stressed that these patterns are only general ones, with a number of exceptions.

Proton transfer barriers

The energy barriers to proton transfer in each of the systems are reported in Table IV. As indicated above, all geometries were optimized at the CIS level (RHF for ground state), including not only the minima in the transfer potential, but also the transition state wherein the proton is approximately halfway between the donor and acceptor atoms. Beginning the discussion with the ground state of malonaldehyde, the CCSD results suggest that the barrier amounts to 4–6 kcal/mol. The barrier is higher by perhaps 2 kcal/mol for the $^3\pi\pi^*$ state; the singlet and triplet $n\pi^*$ states are higher still by another 5–7 kcal/mol, and have very similar barriers to one another.

The DFT barriers reproduce certain aspects of this trend, particularly the higher barriers in the two $n\pi^*$ states, but are quantitatively unreliable. The CIS barriers are quite a bit higher than CCSD, and indicate a much larger difference between the singlet and triplet $n\pi^*$ barriers; moreover the increment between the ground and $^3\pi\pi^*$ states is too large. The CASSCF barriers are higher still and are rather sensitive to choice of active orbitals, indeed erratically so. Incorporation of dynamic correlation dramatically lowers the barriers. The CIS–MP2 barrier for the ground state is slightly lower than the CCSD estimates. The MP2 barriers for the excited states, however, are much too small, lower than the ground state. Similar patterns are noted in the CASPT2 results, only moreso, in that all of the excited states are predicted to have quite negative barriers (i.e., the CASPT2 energy of the CIS transition state geometry is lower than that of the minima).

These energy barriers are illustrated graphically in Fig. 2. It is first immediately obvious that the CASSCF barriers are the highest of all, and there is a great deal of sensitivity to active orbital choice. The (12/13) and (13/13) barriers differ by as much as 10 kcal/mol for the triplets. In contrast, the CASPT2 barriers are the lowest, and retain some of this orbital sensitivity, particularly for the ground state. The CIS barriers follow the same pattern as the CASSCF results, but with lower and more reasonable values. The CIS–MP2 barriers can be seen in Fig. 2 to provide values not too much smaller than the coupled cluster data, although the CCSD pattern of higher barriers for the excited states, compared to S_o, is reversed by CIS–MP2. The DFT results are generally intermediate between CCSD and CIS–MP2.

Including the $^1\pi\pi^*$ state into the analysis, one can summarize that the methods that include dynamic correlation predict lower barriers than do CIS and CASSCF, with the former not quite as high as the latter. All calculations agree that the barrier in the $^1\pi\pi^*$ state is the lowest of all, including the ground state. However, the value of this barrier varies greatly, from highly negative with the CASPT2 procedures to positive with CIS and the (12/13) variant of CASSCF. In fact, the barrier of this state is quite sensitive to the choice of

TABLE IV. Proton transfer barriers (kcal/mol) computed with 6-31+G** basis set.

		CASSCF			CASPT2				
State	CIS	(12/13)	(13/13)	CIS−MP2	(12/13)	(13/13)	DFT	CCSD	CCSD(T)
Malonaldehyde (**M**)									
S_O	10.3	17.3	20.2	2.3	5.1	−1.8	1.5	5.5	4.1
$^1\pi\pi^*$	4.3	12.3	−4.8	−5.8	−18.6	−10.3			
$^3\pi\pi^*$	21.1	39.5	30.2	−0.6	−10.1	−8.0	1.6	7.5	5.4
$^1n\pi^*$	23.7	43.1	40.1	−2.8	−3.8	−3.9	6.1	13.8	10.4
$^3n\pi^*$	28.4	49.4	40.9	0.9	−4.9	−3.2	6.3	14.1	10.9
Diazapentadiene (**D**)									
S_O	16.8	26.7	23.9	8.1	5.7	3.3	6.7	11.2	9.6
$^1\pi\pi^*$	11.0	16.6	1.1	−0.9	−14.2	−1.7			
$^3\pi\pi^*$	27.2	45.0	40.8	6.8	3.7	3.9	9.7	15.5	13.5
$^1n\pi^*$	30.0	44.0	39.5	1.2	6.3	3.8	12.7	18.0	15.4
$^3n\pi^*$	34.8	44.7	38.8	3.5	4.9	3.8	12.3	17.7	15.3
Formimidol (**F**)									
S_O	8.9	15.1	19.5	3.3	3.2	−1.0	1.7		
$^1\pi\pi^*$	6.3	17.2	−11.1	−3.7	−12.3	−5.4			
$^3\pi\pi^*$	24.1	40.4	43.2	0.3	−3.3	−3.1	3.9		
$^1n\pi^*$	29.2	33.2	28.6	9.8	−2.9	0.0			
$^3n\pi^*$	30.1	27.6	20.3	9.3	−12.3	−5.3	13.6		
Glyoxalmonohydrazine ($\mathbf{G_N}$)									
S_O	20.2	33.6	26.3	10.5	9.6	10.3	10.5		
$^1\pi\pi^*$	9.0	4.9	4.4	1.1	1.0	−1.9			
$^3\pi\pi^*$	22.2	19.9	22.1	2.7	6.6	6.4	7.6		
$^1n\pi^*$	8.0	32.5	31.0	6.5	9.5	8.9			
$^3n\pi^*$	3.8	19.7	18.2	2.2	−13.2	−12.3	2.0		
Glyoxalmonohydrazine ($\mathbf{G_O}$)									
S_O	10.5	25.0	16.9	1.5	−0.3	0.7	−1.6		
$^1\pi\pi^*$	3.8	3.8	−8.9	−10.4	−3.7	−12.4			
$^3\pi\pi^*$	20.0	19.2	15.6	−3.5	4.9	5.3	1.4		
$^1n\pi^*$	25.8	22.1	19.6	6.7	30.9	29.4			
$^3n\pi^*$	27.9	31.5	28.9	16.5	22.1	22.2	10.6		

active orbitals in the CASSCF procedure, even after second-order perturbation is included. The barrier computed for the singlet $n\pi^*$ state is not very different than in $^3n\pi^*$.

Patterns of a similar sort can be discerned in the results of the other symmetric systems in Table IV. Just as for malonaldehyde, the transfer barriers in the $^1\pi\pi^*$ state of **D** and **F** are the smallest. Indeed, these barriers are routinely negative for the dynamically correlated methods. The uncorrelated procedures indicate that the barriers of the three other excited states of **M**, **D**, and **F** are all higher than in the ground state, and by a considerable amount. The situation is not so clear cut in the CIS−MP2 and CASPT2 methods where the barriers tend to be somewhat lower for the excited states. As a general rule, the CASSCF barriers are the highest, followed by CIS. Quite a bit lower are the CIS−MP2 barriers, while the CASPT2 values are the lowest. The CASSCF and CASPT2 methods retain a great deal of sensitivity to the nature of the orbitals included in the active space, particularly for the $^1\pi\pi^*$ state. Of the methods tested here (except CCSD), the DFT results are closest in magnitude to CIS−MP2, but by no means do they reproduce them.

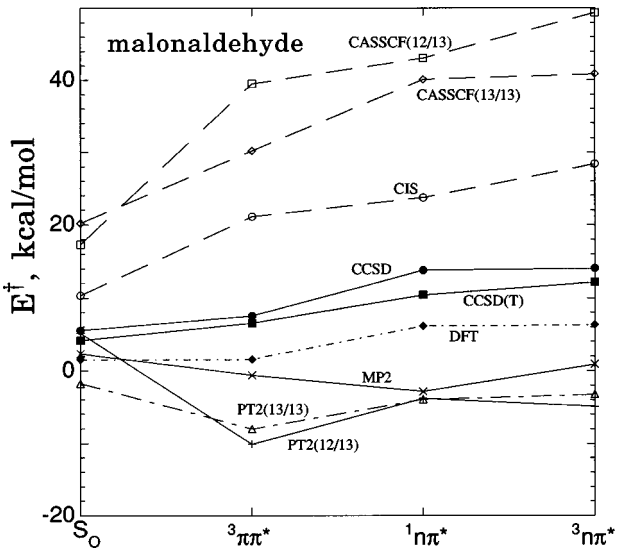

FIG. 2. Proton transfer barriers computed for malonaldehyde at various levels of theory.

Asymmetric system

Unlike the other three systems, the proton transfer potential in glyoxalmonohydrazine is not symmetric. That is, the $\mathbf{G_O}$ and $\mathbf{G_N}$ tautomers are distinct and have different energies. This energy difference is a matter of some importance and varies with the electronic state being considered. The values of ΔE reported in Table V correspond to $E(\mathbf{G_N})-E(\mathbf{G_O})$, such that this quantity is negative when the $\mathbf{G_N}$ tautomer is the more stable of the two.

The first row of data in Table V indicates the ground

TABLE V. Relative energies (kcal/mol) of two tautomers of glyoxalmonohydrazine: $\Delta E = E(\mathbf{G_N}) - E(\mathbf{G_O})$

		CASSCF			CASPT2		
State	CIS	(12/13)	(13/13)	CIS–MP2	(12/13)	(13/13)	DFT
S_O	−9.7	−8.6	−9.4	−9.0	−9.9	−9.6	−12.1
$^1\pi\pi^*$	−5.2	−1.1	−13.3	−11.5	−4.7	−10.5	
$^3\pi\pi^*$	−2.2	−0.7	−6.5	−6.2	−1.7	−1.2	−6.2
$^1n\pi^*$	17.8	−10.4	−11.4	0.2	21.4	20.5	
$^3n\pi^*$	24.1	11.8	10.7	14.3	35.3	34.7	8.6

state value of ΔE is rather well determined, with very little sensitivity to the level of theory: the $\mathbf{G_N}$ tautomer is favored by 9–10 kcal/mol. The situation is quite different for the excited states where the result varies a great deal depending upon the level of theory. Taking the $^3n\pi^*$ state as one example, all the values of ΔE are positive, indicating that $\mathbf{G_O}$ is the favored tautomer. However, the magnitude of ΔE is quite variable. The CIS method predicts a value of 24 kcal/mol, which is lowered to 14 when MP2 correlation is included. In contrast, the CASSCF values are 11–12 kcal/mol, but correlation acts in the opposite way here, to raise these quantities, and by a great deal, all the way up to 35 kcal/mol. The behavior of the $^1n\pi^*$ state is similar in that correlation acts differently upon the CIS and CASSCF values. On the other hand, the values of ΔE are quite a bit smaller for the singlet, some of them less than zero. The values listed for ΔE in Table V for the $\pi\pi^*$ states are all negative so it is likely safe to conclude that $\mathbf{G_N}$ is the favored tautomer, as in the ground state. The magnitude of this preference, however, is variable. Adding correlation to the CIS method intensifies the preference, making ΔE more negative. The result is cloudier for CASSCF since whether the CASPT2 value is more or less negative depends upon the particular set of orbitals chosen.

In summary, all methods agree that $\mathbf{G_N}$ is the favored tautomer in the ground state as well as for the two excited $\pi\pi^*$ states, although the magnitude of this preference is sensitive to theoretical method, and the effect of dynamic correlation is not consistent from one approach to the next. With respect to the $n\pi^*$ states, CASPT2 calculations unambiguously point toward $\mathbf{G_O}$ as the favored tautomer, as does CIS. Uncorrelated CASSCF points toward the opposite conclusion (favoring $\mathbf{G_N}$) for the singlet.

Calculations of a similar sort were also carried out for the 4-31G basis set. The results are remarkably similar to the 6-31+G** data in Table V in many respects. The ground state values of ΔE are again insensitive to level of theory, all leading to an estimate of about −15 or −16 kcal/mol. The latter quantity is more negative than that predicted with the larger set. Indeed, most of the 4-31G estimates of ΔE are more negative than the 6-31+G** predictions, for the excited as well as ground states. The differences between the two basis sets are variable, but can be profound in certain cases. In the $^1n\pi^*$ state, for instance, the CASPT2 result in the penultimate column of Table V is +20.5 kcal/mol. When the 4-31G basis set is substituted, this same quantity reverses sign, becoming −6.0 kcal/mol. One might conclude that the choice of basis set is not an insignificant factor in computing the proton transfer potential of this asymmetric system.

Returning now to the proton transfer barriers, the last two sections of Table IV refer to the difference in energy between the peak of the barrier and the $\mathbf{G_N}$ and $\mathbf{G_O}$ tautomers, respectively. In those cases where ΔE is negative, as is the case for the ground state, and the $\mathbf{G_N}$ tautomer is the more stable of the two, the first, viz. $\mathbf{G_N}$, barrier is of course higher than the $\mathbf{G_O}$ barrier. Many of the patterns noted for the symmetric molecules are repeated here for glyoxalmonohydrizine. The $^1\pi\pi^*$ barriers are generally the smallest for each level of theory, considerably lower than that in the ground state. Electron correlation reduces most of the transfer barriers by quite a bit, both in the comparison between CIS and CIS–MP2, and that between CASSCF and CASPT2. The sensitivity to orbital choice in the CASSCF formalism remains in this asymmetric system.

There are several trends noted in the asymmetric glyoxalmonohydrazine that are distinct from the symmetric systems, and which are initially puzzling. Consider, for example, the negative CASPT2 barriers for the $^3n\pi^*$ state in the last row of the $\mathbf{G_N}$ section of Table IV, making these values even more negative than for the $^1\pi\pi^*$ state. Similarly, the $n\pi^*$ CASPT2 barriers for the $\mathbf{G_O}$ configuration appear anomalously large and positive, in comparison to the symmetric systems. These initially surprising results are rooted in the large asymmetry of the proton transfer potential. As is evident from the CASPT2 entries for ΔE of the $^3n\pi^*$ state in the last row of Table V, the $\mathbf{G_O}$ tautomer is favored over $\mathbf{G_N}$ by some 35 kcal/mol. The deep well in which $\mathbf{G_O}$ is located forces the system to climb a high barrier in order to reach the transition state for proton transfer, explaining in part the high $\mathbf{G_O}$ barriers in Table IV. It is hence clear that any sort of fair comparison between the barriers in the symmetric and asymmetric systems must include some way of accounting for the skewing of the transfer potentials in the latter systems.

In the spirit of Marcus theory, wherein an asymmetric proton transfer potential is treated as a perturbation upon a symmetric system,[59–62] the asymmetrizing perturbation corresponds to the values of ΔE in Table V. One can take an arithmetical average of the forward and reverse proton transfer barriers as an estimate of what the barrier would be in a hypothetical symmetric variant of this molecule, the so-called $E_o^{\dagger}$.[31] The patterns of these averages, listed in Table VI, eliminate some of the anomalies noted in the asymmetric barriers of either $\mathbf{G_N}$ or $\mathbf{G_O}$. As in the case of the symmetric systems in the upper three sections of Table IV, the barrier

TABLE VI. Average proton transfer barriers, $E_O^{\dagger}$ (kcal/mol), in glyoxalmonohydrazine.[a]

		CASSCF			CASPT2		
State	CIS	(12/13)	(13/13)	CIS–MP2	(12/13)	(13/13)	DFT
S_O	15.3	29.3	21.6	6.0	4.6	5.5	4.5
$^1\pi\pi^*$	6.4	4.3	−2.3	−4.6	−1.3	−7.3	
$^3\pi\pi^*$	21.1	19.5	18.8	−0.4	5.7	5.8	4.5
$^1n\pi^*$	16.9	27.6	25.3	6.3	20.2	19.1	
$^3n\pi^*$	15.8	20.6	23.5	9.3	−4.5	5.0	6.3

[a]Computed as arithmetic average of $\mathbf{G_N}$ and $\mathbf{G_O}$ barriers in Table IV.

for the $^1\pi\pi^*$ state is clearly the lowest at all theoretical levels; adding dynamic correlation to either CIS or CASSCF substantially lowers each barrier.

Comparison with past work

Some of the patterns noted here are consistent with earlier calculations, although the latter are not complete enough in and of themselves to draw systematic and definitive conclusions. Taking malonaldehyde as one example, Barone and Adamo[58] had found that the DFT and MP2 barriers of the $^3\pi\pi^*$ state are lower than coupled cluster estimates and that CIS is much higher. Excitation energies and transfer barriers obtained by them for the $^3\pi\pi^*$ and $^3n\pi^*$ states using more extended basis sets are close to 6-31+G** estimates. CASPT2 proton transfer barriers were found to be notably lower than uncorrelated CASSCF values in o-hydroxybenzaldehyde[34] as well as in [2,2′-bipyridine]–3,3′-diol (Ref. 22) and 5-hydroxytropolone.[63] The transfer barrier in the $^1\pi\pi^*$ state of salicylic acid[28] follows the pattern CASSCF>CIS>CASPT2, again consistent with our own findings in the more general case. Similarly, the inclusion of correlation has been shown capable of strongly affecting the relative energies of a pair of tautomers.[22] MP2 correlation has also been shown to reduce transfer barriers in a number of systems.[35,64,65]

With regard to experimental quantities with which the theoretical estimates may be compared, the literature is quite sparse. Most of the work concerns malonaldehyde, particularly its ground state. The barrier height for proton transfer has been estimated from microwave measurements to lie in the range of 4–7 kcal/mol.[66,67] Comparison with the first row of Table IV suggests the CCSD methods are particularly accurate for this quantity. Averaging of thermochemical properties for the closely related acetylacetone[68] yield a similar value of 4 kcal/mol. The measurements of the excited states of malonaldehyde consist largely of tunneling splitting data.[69] A smaller splitting in the $^1n\pi^*$ state, as compared to S_o,[70–72] confirms the computational finding of a higher barrier in this excited state, (although later work questioned this interpretation).[73] Other experimental measurements are consistent with our computational finding that the $^1n\pi^*$ state of malonaldehyde is lower than $^1n\pi^*$.[70,72]

While there is no information on the asymmetric glyoxalmonohydrazine molecule itself, there are a number of studies of larger systems that contain the OH···N intramolecular interaction within the context of one or more aromatic rings. These confirm the computational finding that the proton transfer barrier is much reduced in the $^1\pi\pi^*$ state as compared to S_o (Refs. 74–79) but are unable to provide any quantitative estimates of this small barrier if it exists. The same may be said for larger molecules containing the OH···O intramolecular H-bond common to malonaldehyde.[80–86] A recent study[29] has indicated that the $^1\pi\pi^*$ and $^1n\pi^*$ states can be rather close in energy for molecules related to malonaldehyde, consistent with some of the data in Table III.

SUMMARY

The calculated properties of intramolecular H-bonds in the ground and excited electronic states are rather sensitive to the level of theory used for their study. The methods studied here include the CIS and CASSCF approaches which do not include dynamic correlation, and those that do such as CASPT2, MP2, DFT, and coupled-cluster methods. While all methods yield the same ordering of the various electronic states, there are significant discrepancies between the predicted energy separations. MP2 calculations greatly overestimate excitation energies, as does CIS although to a lesser extent. CASPT2 and DFT values are in good agreement with coupled cluster data. CASSCF excitation energies are roughly similar to CIS and exhibit a surprising degree of sensitivity to the particular choice of orbitals included in the active space in certain cases.

The uncorrelated CASSCF and CIS methods fairly well mirror the pattern of proton transfer barriers in the various excited states predicted by coupled cluster, but provide large overestimates, particularly CASSCF. Moreover, the barriers computed by the latter procedure are notably sensitive to choice of active space. The DFT procedure yields a closer approximation to CCSD, albeit they are underestimated by several kcal/mol. Lower still are the MP2 and CASPT2 values, neither of which can be trusted for quantitative accuracy.

In the case of the unsymmetric glyoxalmonohydrazine, the two tautomers are unequal in energy. The bridging proton prefers association with the N atom in the ground state as well as for the two $\pi\pi^*$ states, although the magnitude of this preference is very sensitive to theoretical method; the effect of dynamic correlation is inconsistent from one approach to the next. CASPT2 and CIS calculations of the $n\pi^*$ states favor $\mathbf{G_O}$, while CASSCF favors $\mathbf{G_N}$ for the singlet. When the asymmetry of the transfer potential is accounted for by an averaging procedure, many of the anomalies noted

in the raw results are eliminated, and the trends become consistent with those observed in the symmetric systems.

ACKNOWLEDGMENTS

We are grateful to L. Adamowicz and M. Forés for helpful discussions.

[1] P. T. Chou, D. McMorrow, T. J. Aartsma, and M. Kasha, J. Phys. Chem. **88**, 4596 (1984).
[2] M. Kasha, Acta Phys. Pol. A **71**, 717 (1987).
[3] A. Douhal and R. Sastre, Chem. Phys. Lett. **219**, 91 (1994).
[4] K. Kuldová, A. Corval, H. P. Trommsdorff, and J. M. Lehn, J. Phys. Chem. A **101**, 6850 (1997).
[5] M. L. Martinez, W. C. Cooper, and P.-T. Chou, Chem. Phys. Lett. **193**, 151 (1992).
[6] T. Werner, G. Woessner, and H. E. A. Kramer, in *Photodegradation and Photostabilization of Coatings*, edited by S. P. Pappas and F. H. Winslow (ACS, Washington, D.C., 1981) Vol. 151, p. 1.
[7] T. Werner, J. Phys. Chem. **83**, 320 (1979).
[8] R. M. Tarkka, X. Zhang, and S. A. Jenekhe, J. Am. Chem. Soc. **118**, 9438 (1996).
[9] *Proton-Transfer Reactions*, edited by E. Caldin and V. Gold (Halsted Press, New York, 1975).
[10] S. Scheiner, Acc. Chem. Res. **27**, 402 (1994).
[11] C.-H. Chu and J.-J. Ho, J. Phys. Chem. **99**, 16590 (1995).
[12] S. Wolfe, C.-K. Kim, K. Yang, N. Weinberg, and Z. Shi, J. Am. Chem. Soc. **117**, 4240 (1995).
[13] J. A. Platts and K. E. Laidig, J. Phys. Chem. **100**, 13455 (1996).
[14] A. Douhal, Ber. Bunsenges. Phys. Chem. **102**, 448 (1998).
[15] D. Marks, P. Prosposito, H. Zhang, and M. Glasbeek, Chem. Phys. Lett. **289**, 535 (1998).
[16] T. Sekikawa, T. Kobayashi, and T. Inabe, J. Phys. Chem. B **101**, 10645 (1997).
[17] S. Nagaoka, S. Yamamoto, and K. Mukai, J. Photochem. Photobiol., A **105**, 29 (1996).
[18] M. Pfeiffer, A. Lau, K. Lenz, and T. Elsaesser, Chem. Phys. Lett. **268**, 258 (1997).
[19] C. Chudoba, E. Riedle, M. Pfeiffer, and T. Elsaesser, Chem. Phys. Lett. **263**, 622 (1996).
[20] D. S. English, K. Das, K. D. Ashby, J. Park, J. W. Petrich, and E. W. Castner, J. Am. Chem. Soc. **119**, 11585 (1997).
[21] F. Lahmani and A. Zehnacker-Rentien, J. Phys. Chem. A **101**, 6141 (1997).
[22] A. L. Sobolewski and L. Adamowicz, Chem. Phys. Lett. **252**, 33 (1996).
[23] W. M. Nau, G. Greiner, H. Rau, M. Olivucci, and M. A. Robb, Ber. Bunsenges. Phys. Chem. **102**, 486 (1998).
[24] W.-H. Fang, J. Am. Chem. Soc. **120**, 7568 (1998).
[25] M. Forés, M. Duran, and M. Solà, Chem. Phys. **234**, 1 (1998).
[26] P. Borowicz, A. Grabowska, A. Les, L. Kaczmarek, and B. Zagrodzki, Chem. Phys. Lett. **291**, 351 (1998).
[27] J. J. Paz, M. Moreno, and J. M. Lluch, J. Chem. Phys. **108**, 8114 (1998).
[28] A. L. Sobolewski and W. Domcke, Chem. Phys. **232**, 257 (1998).
[29] S. Tobita, M. Yamamoto, N. Kurahayashi, R. Tsukagoshi, Y. Nakamura, and H. Shizuka, J. Phys. Chem. A **102**, 5206 (1998).
[30] M. A. Ríos and M. C. Ríos, J. Phys. Chem. A **102**, 1560 (1998).
[31] M. Cuma, S. Scheiner, and T. Kar, J. Mol. Struct.: THEOCHEM (in press).
[32] S. Scheiner, T. Kar, and M. Cuma, J. Phys. Chem. A **101**, 5901 (1997).
[33] S. Nagaoka and U. Nagashima, Chem. Phys. **136**, 153 (1989).
[34] A. L. Sobolewski and W. Domcke, Chem. Phys. **184**, 115 (1994).
[35] K. Luth and S. Scheiner, J. Phys. Chem. **98**, 3582 (1994).
[36] M. C. Rovira, and S. Scheiner, J. Phys. Chem. **99**, 9854 (1995).
[37] M. Cuma, C. Thompson, and S. Scheiner, J. Comput. Chem. **19**, 129 (1998).
[38] K. Luth and S. Scheiner, J. Phys. Chem. **99**, 7352 (1995).
[39] R. Ditchfield, W. J. Hehre, and J. A. Pople, J. Chem. Phys. **54**, 724 (1971).
[40] R. Krishnan, J. S. Binkley, R. Seeger, and J. A. Pople, J. Chem. Phys. **72**, 650 (1980).
[41] T. Clark, J. Chandrasekhar, G. W. Spitznagel, and P. v. R. Schleyer, J. Comput. Chem. **4**, 294 (1983).
[42] J. B. Foresman, M. Head-Gordon, J. A. Pople, and M. J. Frisch, J. Phys. Chem. **96**, 135 (1992).
[43] B. O. Roos, in *Ab Initio Methods in Quantum Chemistry*, edited by K. P. Lawley (Wiley, New York, 1987) Vol. 2, p. 399.
[44] B. O. Roos, P. Linse, P. E. M. Siegbahn, and M. R. A. Blomberg, Chem. Phys. **66**, 197 (1981).
[45] K. Andersson, P. Malmqvist, B. O. Roos, A. J. Sadlej, and K. Wolinski, J. Phys. Chem. **94**, 5483 (1990).
[46] K. Andersson, P. Malmqvist, and B. O. Roos, J. Chem. Phys. **96**, 1218 (1992).
[47] K. Andersson, M. R. A. Blomberg, M. P. Fulscher, G. Karlstrom, V. Kello, R. Lindh, P.-A. Malmqvist, J. Noga, J. Olsen, B. O. Roos, A. J. Sadlej, P. E. M. Siegbahn, M. Urban, and P.-O. Widmark, MOLCAS-3 (University of Lund, Sweden, 1994).
[48] J. Cizek, Adv. Chem. Phys. **14**, 35 (1969).
[49] G. D. Purvis and R. J. Bartlett, J. Chem. Phys. **76**, 1910 (1982).
[50] G. E. Scuseria and H. F. Schaefer, J. Chem. Phys. **90**, 3700 (1989).
[51] J. A. Pople, M. Head-Gordon, and K. Raghavachari, J. Chem. Phys. **87**, 5968 (1987).
[52] *Density Functional Methods in Chemistry*, edited by J. Labanowski and J. Andzelm (Springer, New York, 1991).
[53] A. St-Amant, in *Reviews in Computational Chemistry*, edited by D. Boyd and K. Lipkowitz (VCH, New York, 1996) Vol. 7, p. 217.
[54] A. D. Becke, J. Chem. Phys. **98**, 5648 (1993).
[55] C. Lee, W. Yang, and R. G. Parr, Phys. Rev. B **37**, 785 (1988).
[56] GAUSSIAN 94, M. J. Frisch, G. W. Trucks, H. B. Schlegel, P. M. W. Gill, B. G. Johnson, M. A. Robb, J. R. Cheeseman, T. A. Keith, G. A. Petersson, J. A. Montgomery, K. Raghavachari, M. A. Al-Laham, V. G. Zakrzewski, J. V. Ortiz, J. B. Foresman, J. Cioslowski, B. B. Stefanov, A. Nanayakkara, M. Challacombe, C. Y. Peng, P. Y. Ayala, W. Chen, M. W. Wong, J. L. Andres, E. S. Replogle, R. Gomperts, R. L. Martin, D. J. Fox, J. S. Binkley, D. J. Defrees, J. J. P. Stewart, M. Head-Gordon, G. Gonzalez, and J. A. Pople, Gaussian, Inc., Pittsburgh, PA, 1995.
[57] GAUSSIAN 98, Revision A.6, M. J. Frisch, G. W. Trucks, H. B. Schlegel, G. E. Scuseria, M. A. Robb, J. R. Cheeseman, V. G. Zakrzewski, J. A. Montgomery, R. E. Stratmann, J. C. Burant, S. Dapprich, J. M. Millam, A. D. Daniels, K. N. Kudin, M. C. Strain, O. Farkas, J. Tomasi, V. Barone, M. Cossi, R. Cammi, B. Mennucci, C. Pomelli, C. Adamo, S. Clifford, J. Ochterski, G. A. Petersson, P. Y. Ayala, Q. Cui, K. Morokuma, D. K. Malick, A. D. Rabuck, K. Raghavachari, J. B. Foresman, J. Cioslowski, J. V. Ortiz, B. B. Stefanov, G. Liu, A. Liashenko, P. Piskorz, I. Komaromi, R. Gomperts, R. L. Martin, D. J. Fox, T. Keith, M. A. Al-Laham, C. Y. Peng, A. Nanayakkara, C. Gonzalez, M. Challacombe, P. M. W. Gill, B. Johnson, W. Chen, M. W. Wong, J. L. Andres, C. Gonzalez, M. Head-Gordon, E. S. Replogle and J. A. Pople, Gaussian, Inc., Pittsburgh, PA, 1998.
[58] V. Barone and C. Adamo, J. Chem. Phys. **105**, 11007 (1996).
[59] R. A. Marcus, Annu. Rev. Phys. Chem. **15**, 155 (1964).
[60] R. A. Marcus, J. Phys. Chem. **72**, 891 (1968).
[61] W. J. Albery, Annu. Rev. Phys. Chem. **31**, 227 (1980).
[62] S. Scheiner and P. Redfern, J. Phys. Chem. **90**, 2969 (1986).
[63] J. J. Paz, M. Moreno, and J. M. Lluch, J. Chem. Phys. **107**, 6275 (1997).
[64] V. Guallar, M. Moreno, J. M. Lluch, F. Amat-Guerri, and A. Douhal, J. Phys. Chem. **100**, 19789 (1996).
[65] X. Duan and S. Scheiner, Chem. Phys. Lett. **204**, 36 (1993).
[66] S. L. Baughcum, Z. Smith, E. B. Wilson, and R. W. Duerst, J. Am. Chem. Soc. **106**, 2260 (1984).
[67] D. W. Firth, K. Beyer, M. A. Dvorak, S. W. Reeve, A. Grushow, and K. R. Leopold, J. Chem. Phys. **94**, 1812 (1991).
[68] S. H. Bauer and C. F. Wilcox, Chem. Phys. Lett. **279**, 122 (1997).
[69] D. W. Firth, P. F. Barbara, and H. P. Trommsdorff, Chem. Phys. **136**, 349 (1989).
[70] C. J. Seliskar and R. E. Hoffmann, Chem. Phys. Lett. **43**, 481 (1976).
[71] C. J. Seliskar and R. E. Hoffmann, J. Am. Chem. Soc. **99**, 7072 (1977).
[72] C. J. Seliskar and R. E. Hoffmann, J. Mol. Spectrosc. **88**, 30 (1981).
[73] A. A. Arias, T. A. W. Wasserman, and P. H. Vaccaro, J. Chem. Phys. **107**, 5617 (1997).
[74] A. Mordzinski and W. Kühnle, J. Phys. Chem. **90**, 1455 (1986).
[75] N. P. Ernsting, A. Mordzinski, and B. Dick, J. Phys. Chem. **91**, 1404 (1987).
[76] F. Laermer, T. Elsaesser, and W. Kaiser, Chem. Phys. Lett. **148**, 119 (1988).
[77] A. Douhal, F. Lahmani, A. Zehnacker-Rentien, and F. Amat-Guerri, J. Phys. Chem. **98**, 12198 (1994).

[78] C. Chudoba, S. Lutgen, T. Jentzsch, E. Riedle, M. Woerner, and T. Elsaesser, Chem. Phys. Lett. **240**, 35 (1995).
[79] M. Mosquera, J. C. Penedo, M. C. R. Rodríguez, and F. Rodríguez-Prieto, J. Phys. Chem. **100**, 5398 (1996).
[80] Y. Tomioka, M. Ito, and N. Mikami, J. Phys. Chem. **87**, 4401 (1983).
[81] D. McMorrow and M. Kasha, J. Phys. Chem. **88**, 2235 (1984).
[82] S. L. Studer, P. T. Chou, and D. McMorrow, Chem. Phys. Lett. **161**, 361 (1989).
[83] P.-T. Chou, M. L. Martinez, and S. L. Studer, J. Phys. Chem. **94**, 3639 (1990).
[84] T. Tsuji, H. Sekiya, Y. Nishimura, R. Mori, A. Mori, and H. Takeshita, J. Chem. Phys. **97**, 6032 (1992).
[85] S. Nagaoka, Y. Shinde, K. Mukai, and U. Nagashima, J. Phys. Chem. A **101**, 3061 (1997).
[86] K. B. Andersen and J. Spanget-Larsen, Spectrochim. Acta A **53**, 2615 (1997).